Supplementary Figure 1:

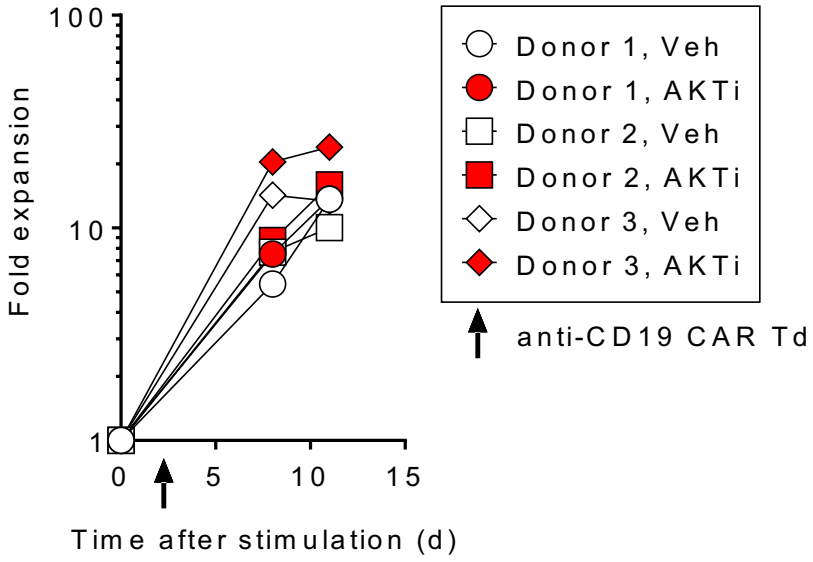

Supplemental Figure 1. **Growth rate kinetics of PBMC stimulated with anti-CD3 and transduced with an anti-CD19 CAR in the presence of AKTi or vehicle control**. PBMC from *n* = 3 independently evaluated healthy donors was stimulated with anti-CD3 (50 ng mL^{-1}) in the continuous presence of IL-2 (300 IU/mL) and AKTi (1 μM) or a vehicle control (Veh). On D+2, cells underwent a single round of retroviral transduction with an anti-CD19 CAR.

Supplementary Figure 2

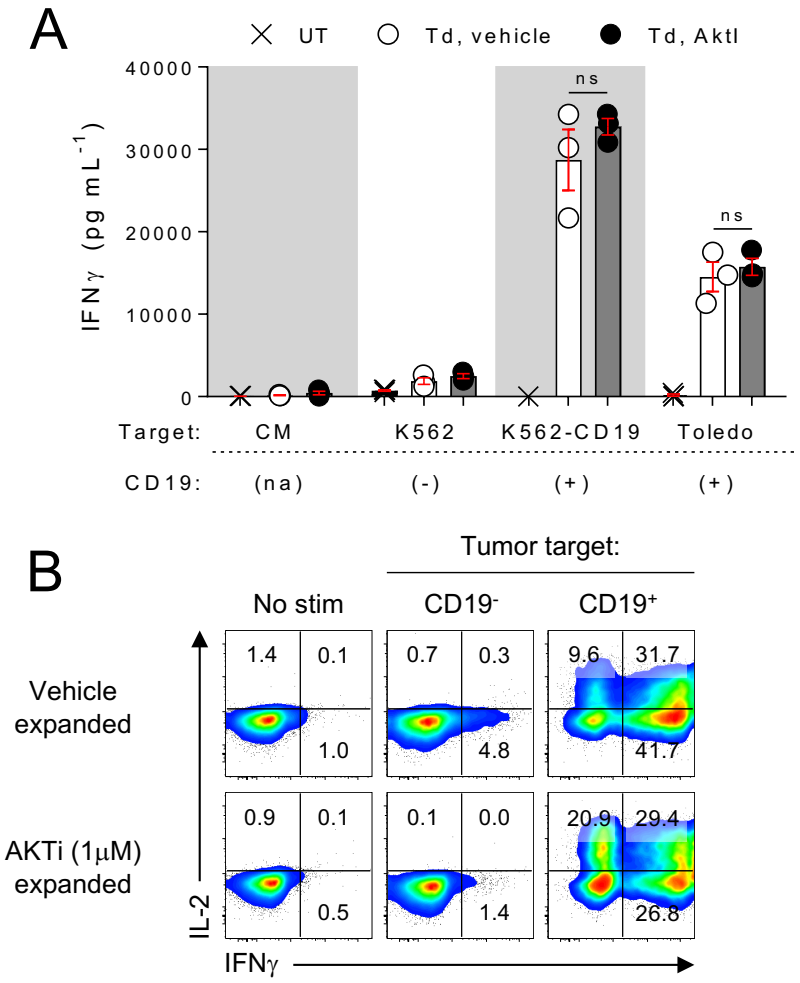

Supplemental Figure 2. **Expansion of anti-CD19 CAR modified human peripheral blood T cells in the presence of a pharmacologic AKT inhibitor does not impair antigen-specific IFNγ release**. (**A**) Peripheral blood mononuclear cells were stimulated with OKT3 (50 ng mL^{-1}) and IL-2 (300 IU mL^{-1}) in the continuous presence of AKTi (1μM) or a vehicle control. Stimulated T cells underwent retroviral transduction (Td) with an anti-CD19 CAR on d(+)2 or were left untransduced (UT) as controls. Cells were expanded for a total of 10d, harvested, washed 3 times, and then plated overnight alone or in a 1:1 mixture with indicated target cell lines in culture media (CM) free of both cytokines and AKTi. Results are presented as mean ± SEM and individual measurements using modified T cells generated from *n* = 3 independently evaluated patient donors. Statistical comparison performed using an unpaired 2-tailed Student's t test; ns = not significant. n.a. = not applicable. (**B**) Intracellular IFNγ and IL-2 staining assessed by FACS in anti-CD19 CAR modified T cells expanded in the presence of AKTi or vehicle control and co-cultured for 6h in AKTi-free CM alone or with a 1:2 mixture with CD19$^-$ (K562) or CD19$^+$ (143B-CD19) tumor cells. Data shown after gating on viable singlet lymphocytes. Results from one of three representative experiments using cells derived from healthy donors is shown.

Supplementary Figure 3:

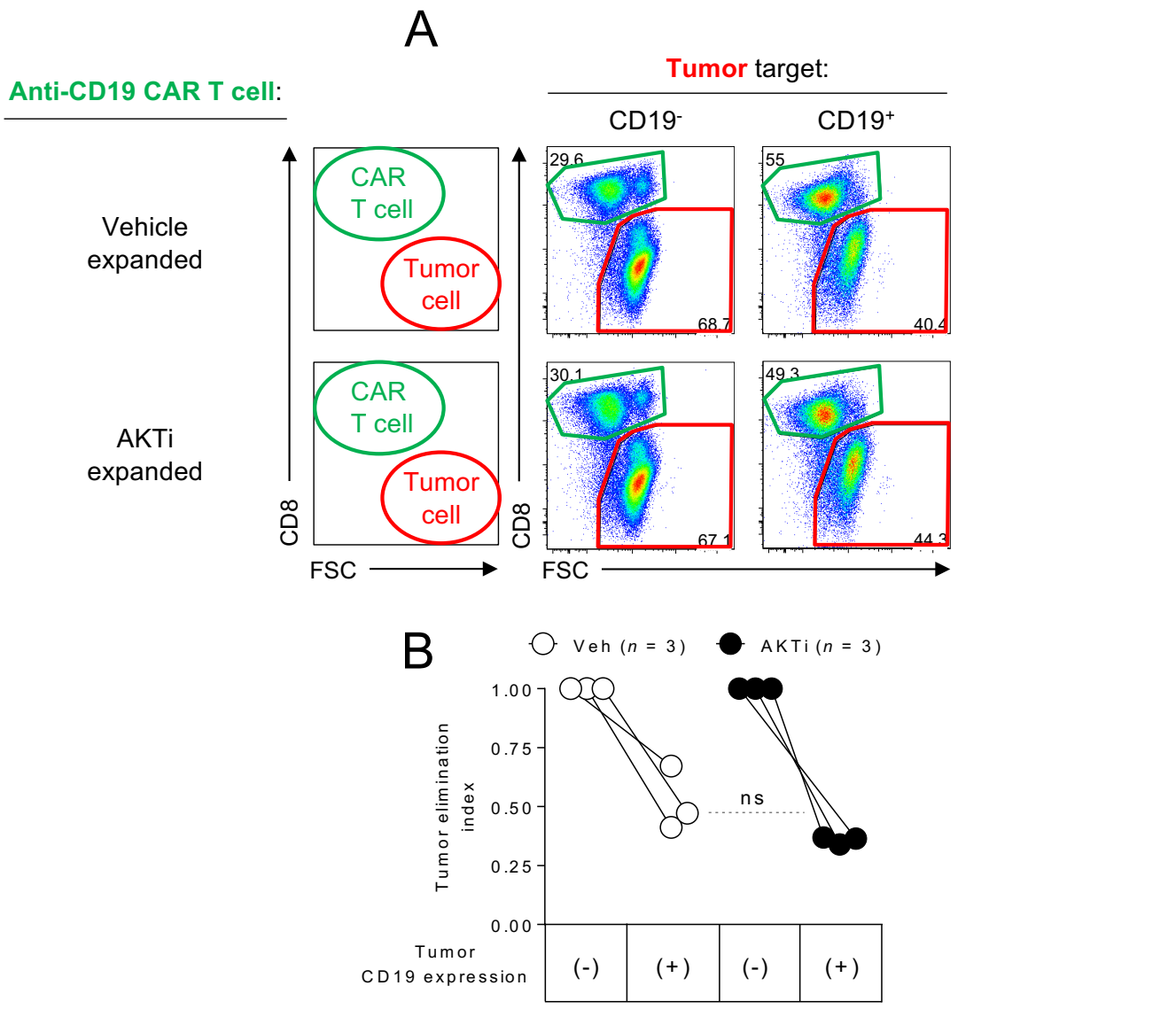

Supplemental Figure 3. Anti-CD19 CAR modified T cells expanded in AKTi eliminate tumor cells in an antigen-specific manner. (**A**) Representative FACS plots and (**B**) summary graph measuring the ability of anti-CD19 CAR modified T cells expanded in the presence or absence of AKTi to eliminate tumor cells in an antigen specific manner. T cells were from *n* = 3 independently evaluated healthy donors were activated, transduced with the anti-CD19 CAR, and expanded for 10d in the continuous presence of IL-2 (300 IU mL^{-1}), AKTi (1μM) or vehicle control. Modified T cells were then washed and co-cultured for 6h in AKTi-free CM in a 1:2 mixture with $CD19^-$ (K562) or $CD19^+$ (143B-CD19) tumor cells. The tumor elimination index was calculated as described in the Methods Section. Statistical comparison performed using an unpaired 2-tailed Student's t test; ns = not significant.

Supplementary Figure 4:

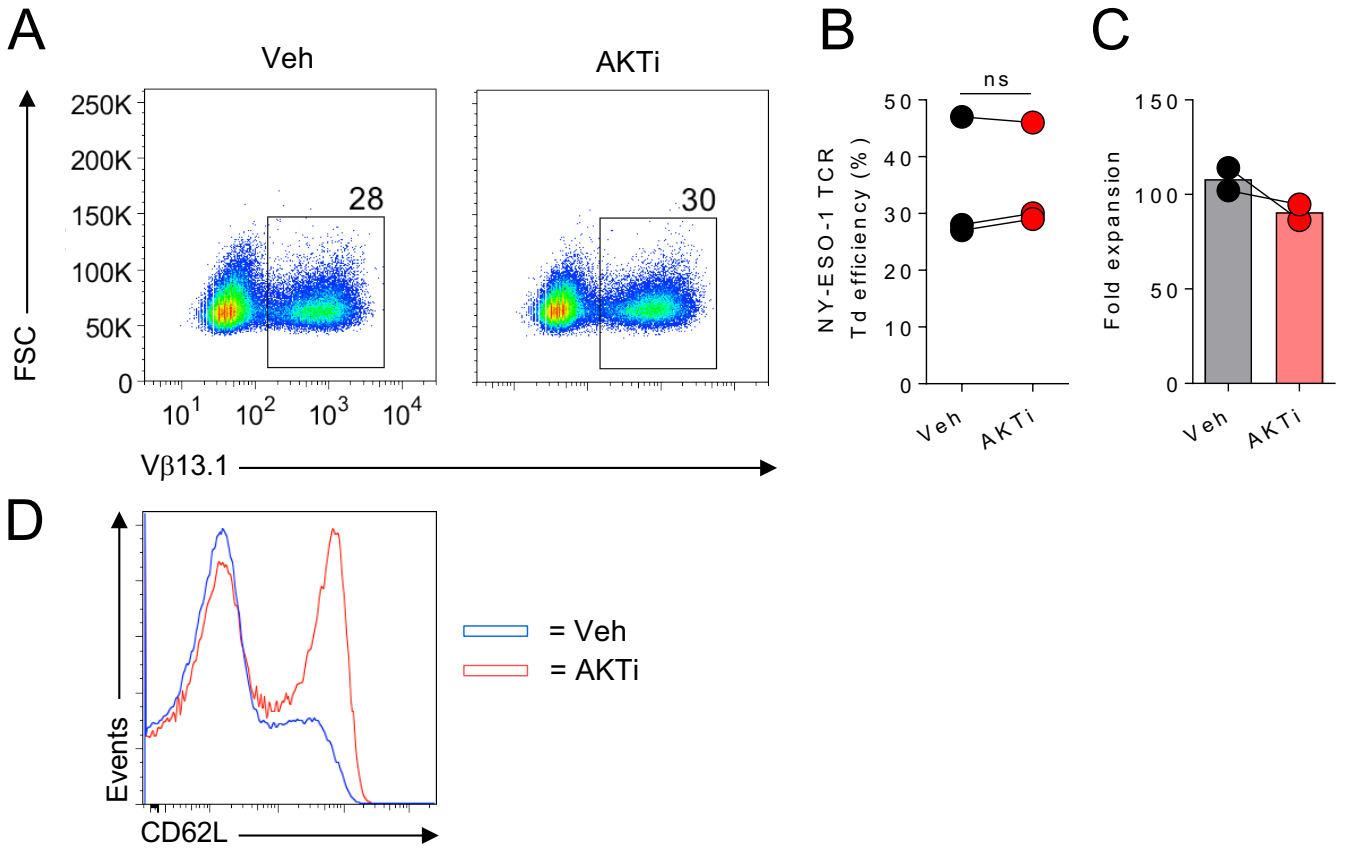

Supplemental Figure 4: Inhibition of AKT does not impair the transduction efficiency of a TCR specific for the cancer-germline antigen NY-ESO-1. (A) Representative FACS plots and **(B)** summary graph demonstrating the retroviral transduction efficiency (as measured by Vβ13.1 expression) of the NY-ESO-1 TCR in peripheral blood lymphocytes from *n* = 3 independent donors with metastatic melanoma expanded in the presence of AKTi (1μM) or Vehicle control (Veh) and IL-2 (300 IU mL^{-1}). (**C**) Fold expansion of NY-ESO-1 TCR transduced T cells expanded for 10d in AKTi or Veh from *n* = 2 independent donors. (**D**) Representative FACS plot demonstrating the expression of CD62L on NY-ESO-1 TCR engineered cells expanded in the presence of AKTi or Veh control. Similar results were obtained in 3 independent experiments. All FACS data shown after gating on $live^+CD3^+$ lymphocytes. Statistical comparison performed using an unpaired 2-tailed Student's t test; ns = not significant.

Supplementary Figure 5:

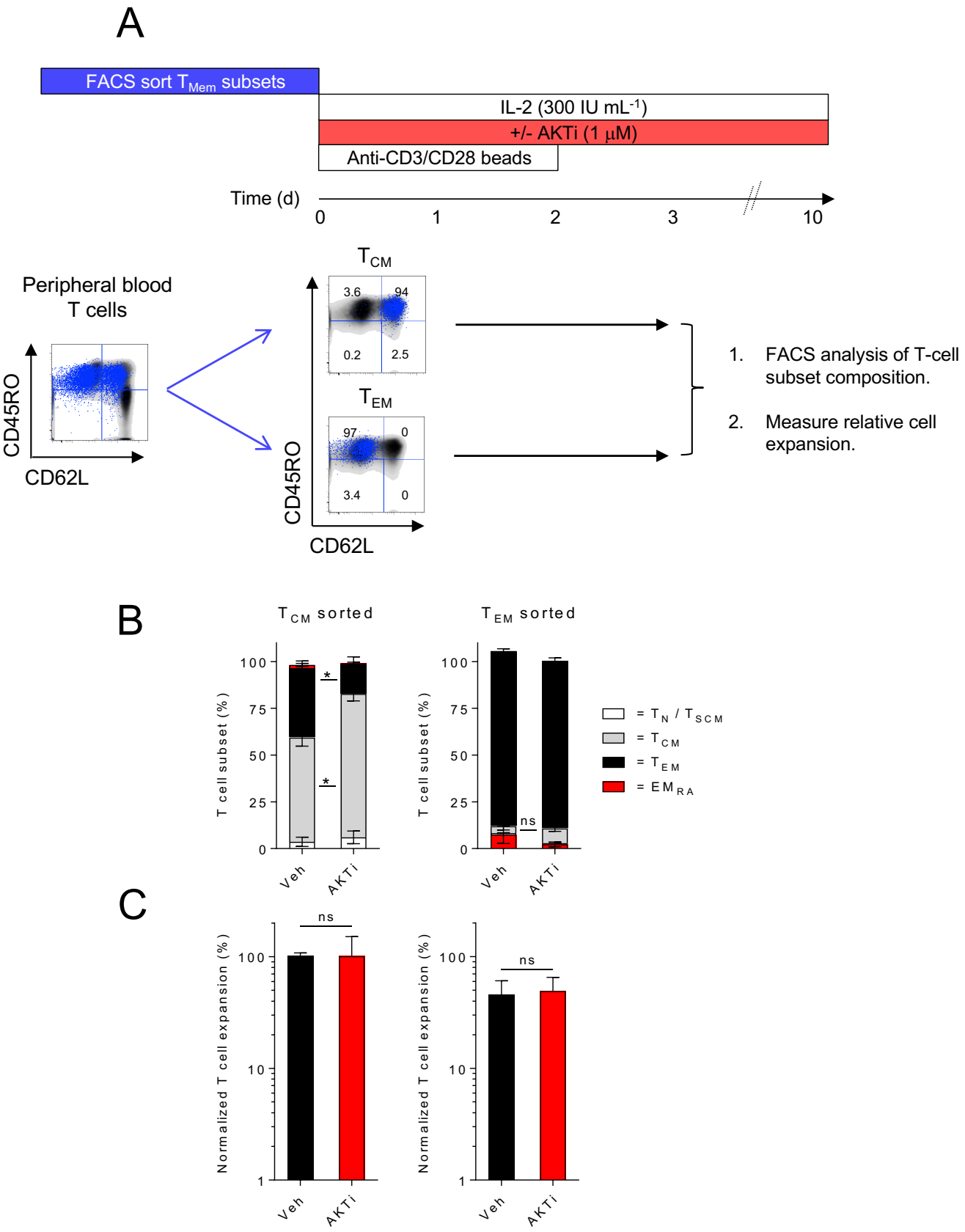

Supplemental Figure 5: AKT inhibition promotes expansion of CD62L-expressing T_{CM}-derived cells following stimulation with anti-CD3/CD28 microbeads. (**A**) Schematic overview of the isolation by FACS-sort of T_{CM} and T_{EM} subsets from the peripheral blood followed by activation with anti-CD3/CD28 microbeads in the continuous presence of IL-2 (300 IU mL^{-1}) and AKTi (1 μM) or vehicle control. (**B**) Resulting subset composition and (**C**) relative cell expansion of isolated T_{CM} or T_{EM} cells expanded for 10d. Summary of results using T cells isolated from $n = 4$ (T_{CM}) and $n = 3$ (T_{EM}) independently evaluated healthy donors is shown as mean ± SEM. Statistical comparisons performed using an unpaired 2-tailed Student's t test; $^*P < 0.05$, ns = not significant.

Supplementary Figure 6:

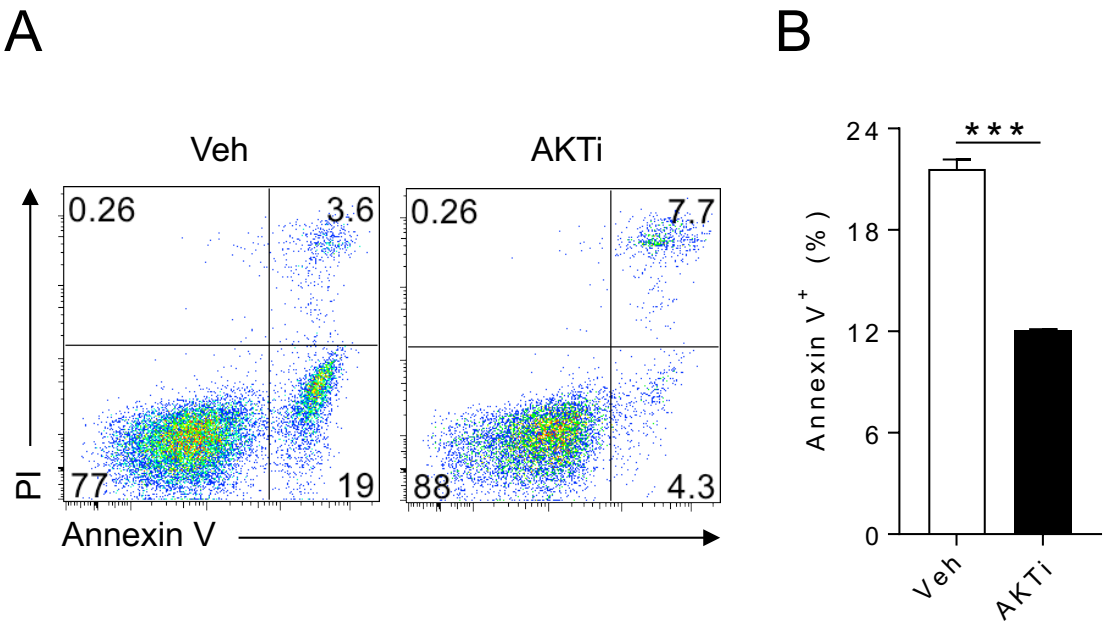

Supplemental Figure 6. **Inhibition of AKT limits activation-induced cell death in T cells expanded from peripheral blood. (A)** Representative FACS plot and **(B)** summary graph demonstrating the frequency of annexin$^+$ T cells 10d after expansion in the continuous presence of IL-2 (300 IU mL^{-1}) and AKTi (1μM) or Vehicle control (Veh). Data is shown after gating on CD3$^+$ lymphocytes and is representative of n = 3 independently performed experiments using patient-derived T cells. Results in panel **B** is presented as mean ± SEM with n = 3 replicates with a statistical comparison performed using an unpaired 2-tailed Student's t test. ***P < 0.001.

Supplementary Figure 7:

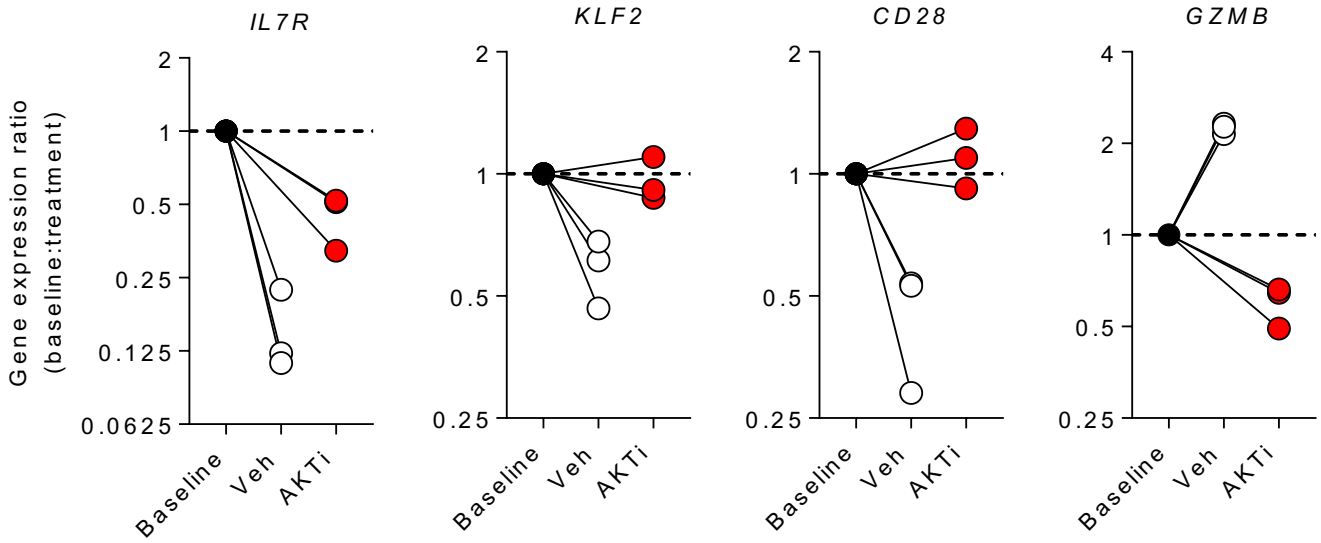

Supplemental Figure 7. **AKTi minimizes changes to key differentiation associated genes during *ex vivo* cell expansion.** Comparison of gene expression for *IL7R*, *KLF2*, *CD28*, and *GZMB* in anti-CD19 CAR modified T cells expanded in AKTi (1μM) or Veh control relative to expression in a matched starting population of peripheral blood T cells. Horizontal dashed lines represent a ratio of 1 (no change in gene expression). Results from *n* = 3 independently evaluated patient donors is shown.

Supplementary Figure 8:

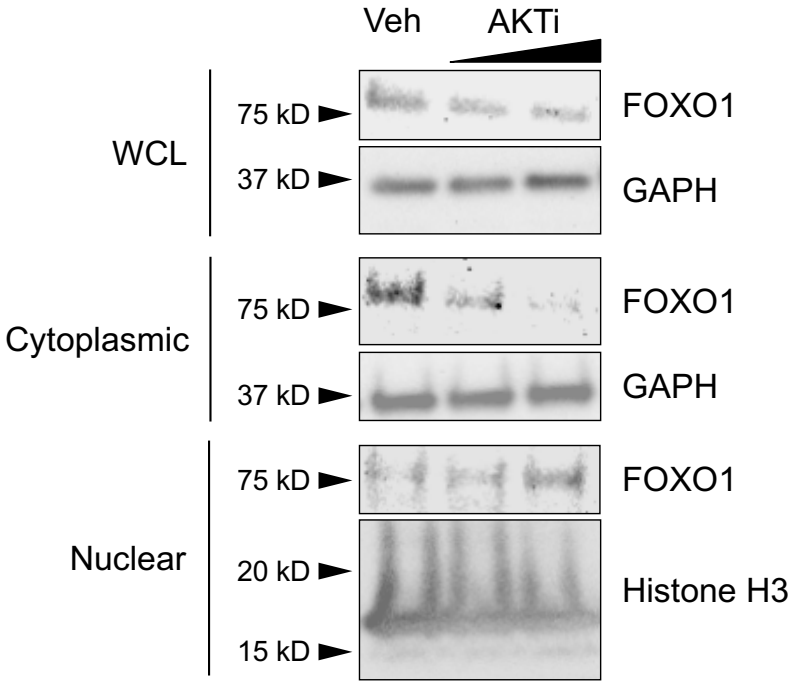

Supplemental Figure 8. **AKTi enforces nuclear and minimizes cytoplasmic localization of FOXO1 in activated human T cells.** $CD3^+$ T cells obtained by magnetic bead isolation from the peripheral blood of a healthy donor were stimulated with plate bound anti-CD3/CD28 (1μg) in the presence of IL-2 (300 IU mL-1) and AKTi (1 and 3.3 μM) or vehicle control for 5d. Protein from different subcellular compartments was extracted using a Cell Fractionation Kit prior to loading a normalized quantity of protein onto a 4-20% gradient gel under reducing conditions. After electrophoresis, protein was transferred onto a polyvinylidene difluoride membrane, blocked for 1h, followed by overnight incubation at 4^oC in primary antibodies against indicated proteins. The following day, the blots were incubated for 1h in either goat-anti-rabbit horse-radish peroxidase (HRP) or goat-anti-mouse HRP secondary antibodies. Enhanced chemiluminescence substrate was added immediately before blot development. Results from one of two representative experiments is shown. WCL = whole cell lysate.

Supplementary Figure 9:

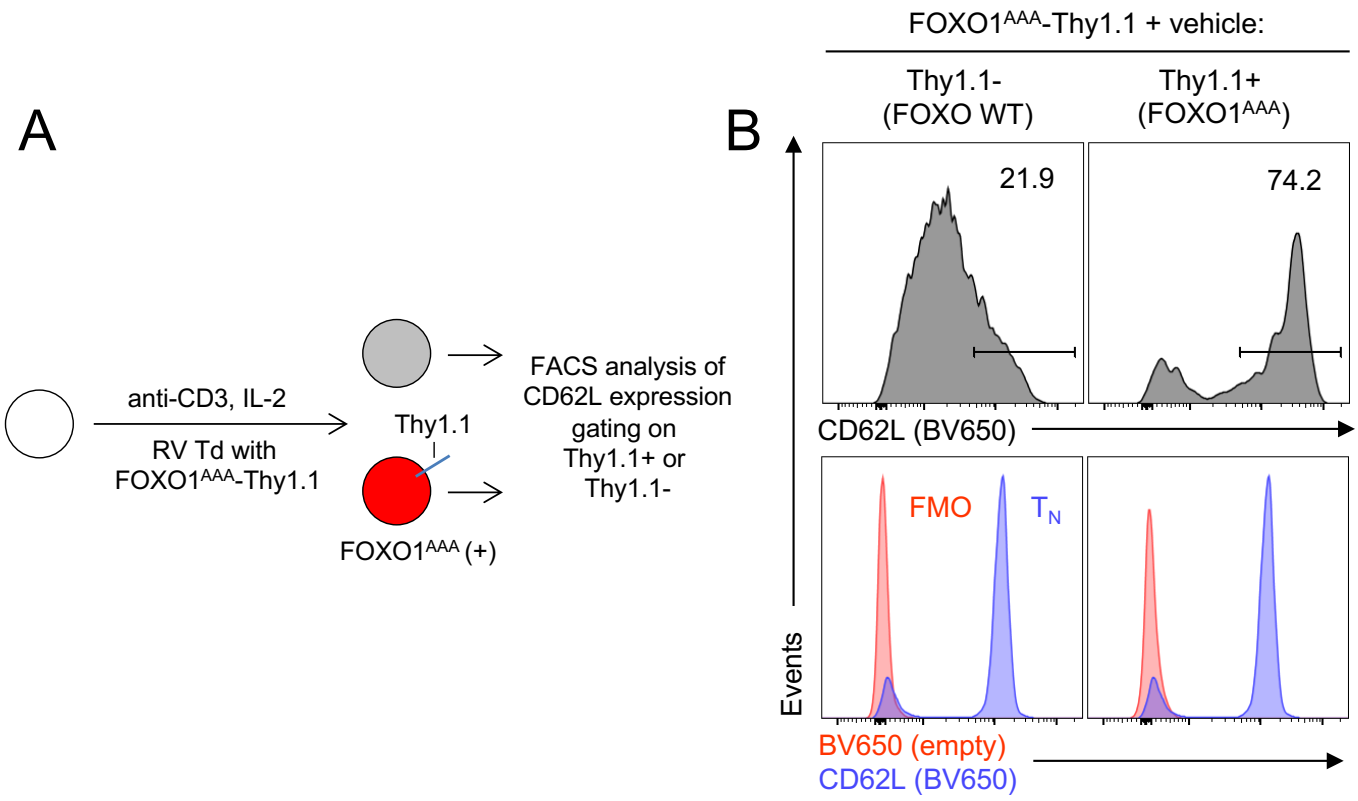

Supplemental Figure 9: Constitutively active FOXO1^{AAA} upregulates CD62L in a cell intrinsic manner. (**A**) Schema for the stimulation of human PBMC with anti-CD3 (50 ng mL^{-1}), retroviral transduction (RV Td) with FOXO1^{AAA}-Thy1.1, expansion in IL-2 (300 IU mL^{-1}), and analysis by FACS. (**B**) Expression of CD62L on T cells from the same culture gated on a Thy1.1^{-} and Thy1.1^{+} population 5d after stimulation and retroviral transduction with the FOXO1^{AAA}-Thy1.1 construct. Results after gating on live^{+}singlet^{+}CD8^{+} cells from one of three representative experiments using HD T cells is shown. Gating for CD62L was based on both a fluorescence minus one (FMO) negative control and the staining of unstimulated naïve T cells from the peripheral blood as a positive control, as shown.

Supplementary Figure 10:

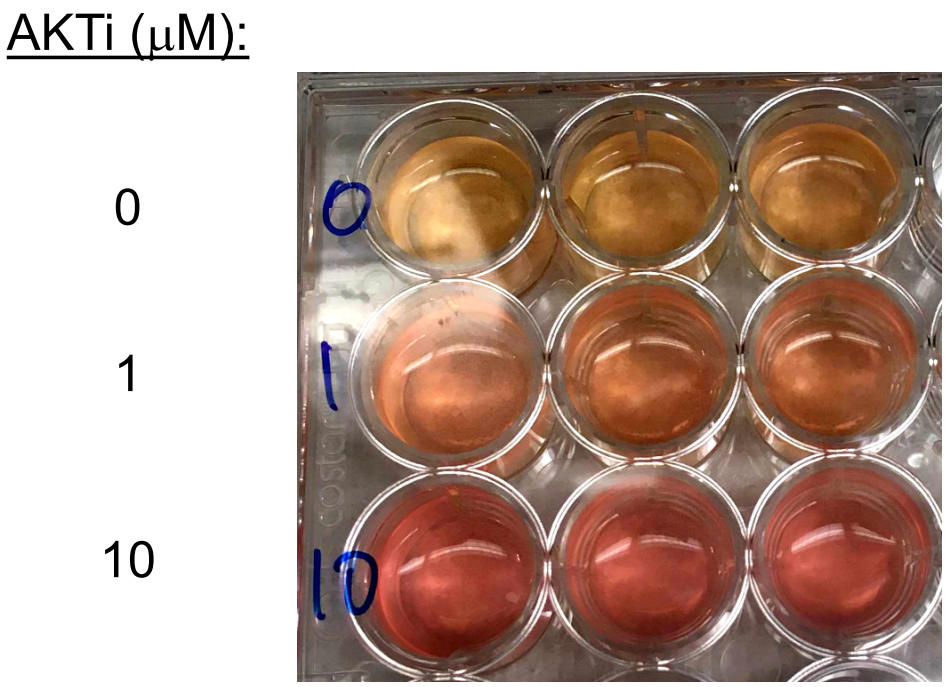

Supplemental Figure 10. **AKTi causes dose-dependent suppression of culture media acidification**. Comparison of culture media acidification using the acid-base indicator phenol red in peripheral blood T cells 5 days after activation in the presence of titrated concentrations of AKTi or vehicle control. Yellow color indicates acidification while red indicates alkaline media. Representative culture results from one of six patient and healthy donors is shown.

Supplementary Figure 11:

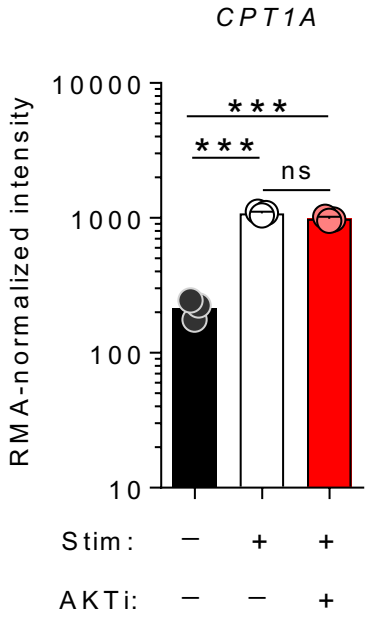

Supplemental Figure 11. **AKTi does not alter the expression of *CPT1A* in CD19 CAR engineered T cells.** Expression of the gene encoding carnitine palmitoyltransferase 1a (*CPT1A)*, a rate-limiting enzyme involved in fatty acid oxidation, in peripheral blood lymphocytes at rest and 10d following activation, retroviral transduction, and expansion in AKTi (1μM) or vehicle control. Results are presented as the mean ± SEM from *n* = 3 independently evaluated patient donors. Statistical analysis performed using an unpaired 2-tailed Student's t test corrected for multiple comparisons by a Bonferroni adjustment. ****P* < 0.001; ns = not significant.

Supplementary Figure 12:

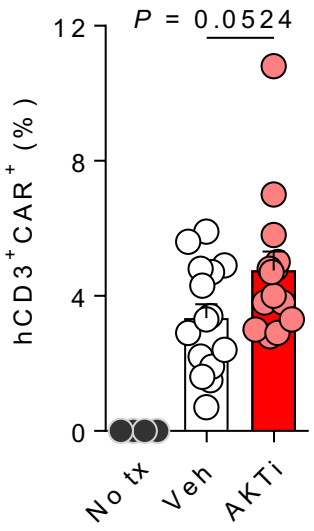

Supplemental Figure 12. **AKTi is not associated with significantly increased CAR T cell persistence at a late time point.** Evaluation of the frequency of human $CD3^{+}CAR^{+}$ T cells in the spleens of immune-deficient NSG mice 30d following adoptive transfer of 1 x 10^{6} anti-CD19 CAR transduced patient-derived T cells expanded in the presence of AKTi or vehicle (Veh) control. T cells were administered by i.v injection without additional cytokine support. An equal number of NSG mice were left untreated as controls. Infused mice received anti-CD19 CAR transduced human T cells from one of three patient donors (*n* = 5 mice/donor/cell expansion condition; total *n* per condition = 15). Pooled results using cells from all 3 donors are presented as mean ± SEM. Statistical analysis performed using an unpaired 2-tailed Student's t test with the resultant *P* value displayed.